Organic & Biomolecular Chemistry

COMMUNICATION

View Article Online
View Journal | View Issue

Cite this: *Org. Biomol. Chem.*, 2019, **17**, 9573

Received 26th July 2019,
Accepted 28th October 2019

DOI: 10.1039/c9ob01649j

rsc.li/obc

Chiral bisphosphine ligands based on quinoline oligoamide foldamers: application in asymmetric hydrogenation†

Lu Zheng,[a,b,c] Dan Zheng,[d] Yanru Wang,[d] Chengyuan Yu,[d] Kun Zhang*[a,b] and Hua Jiang *[a,b,d]

A series of chiral bisphosphine ligands were designed and synthesized based on single-handed quinoline oligoamide foldamers. The bisphosphine ligands can coordinate with $Rh(cod)_2BF_4$ in a 1 : 1 stoichiometry and the resulted chiral Rh(I) catalysts were applied in the asymmetric hydrogenation of α-dehydroamino acid esters, in which excellent conversions and promising levels of enantioselectivity were achieved.

The functions of biopolymers highly rely on their structures, such as the helical structure of DNA, peptides and proteins. A lot of well-defined folded structures have been developed in recent years to mimic the conformation of helical biopolymers but the reports that mimic the function of helical structures is rather few.[1] Inspired by the high catalytic activity and selectivity of enzyme catalysis under mild conditions,[2,3] foldamer-based catalysis is considered as a promising area that has the advantage of enzyme catalysis and a wide scope of application, but it is still at an infant stage. Huc[4,5] and Moore[6,7] have reported several prominent examples that foldamers enhance reaction rates but the reports about foldamer-based asymmetric catalysis are rather limited.[8] Artificial helical structures have been developed in recent years to mimic the properties of DNA and peptides[2,9,10] and some helical polymer-based structures have been used as scaffolds for asymmetric catalysis because they are expected to have a huge steric hindrance compared with small-molecule-based chiral structures and the enantioselectivity of this kind of catalyst mainly originates from the main chain chirality or the chiral pendants such as the chiral active sites or metal-binding sites.[11–14] By contrast, increasing attention is being paid to catalysts whose enantiodiscrimination relies on the main chain chirality because it only requires the introduction of a simple achiral ligand or catalyst. Recently, Suginome has developed several chiral poly(quinoxaline-2,3-diyl)-based phosphines (PQXphos) as helical macromolecular ligands for some asymmetric reactions and excellent conversions and enantioselectivities have been observed.[15–19] Some helical-shaped small molecules such as helicenes and their derivatives, some octahedral metal complexes and certain axially chiral biaryl systems are also used as asymmetric catalysts,[20,21] but the asymmetric catalysis based on foldamers is still a huge challenge.[22]

Quinoline oligoamide foldamers (QOFs) composed of achiral repeating units exhibit interconvertible equilibrium between the left (*M*)-handed and right (*P*)-handed enantiomers.[23] Attaching a chiral moiety to the terminus of the foldamer is one of the major methods to achieve absolute control of the helix sense, which leads to potential applications in chiral recognition and chiral electro-optical devices. Huc and our group have reported several chiral moieties that can absolutely bias QOFs to a one-handed helix with high fidelity which renders QOFs to be good chiral scaffolds for asymmetric catalysis.[24–26] The crystal structure of quinoline oligoamide foldamers shows that the helical structure comprises 2.5 repeat units per turn and the C-terminus and the side chain of the third monomer (from the C-terminus) are on the same face of the foldamer, which bring them in close proximity and thus provide a chance to be locked through a covalent bond.[23,27] In this work, we propose to modify the C-terminus and the side chain of single-handed quinoline oligoamide foldamers with phosphorus groups to provide several bisphosphine ligands and to investigate whether these ligands can be used as a catalytic platform for metal-catalyzed asymmetric reactions (Fig. 1). For the asymmetric reaction, we chose rhodium-catalyzed asymmetric hydrogenation of α-dehydroamino acid esters as the model.

Phosphine ligands, such as chiral diphosphines, P- and N-ligands, and monodentate phosphorus ligands, are one of

[a]*School of Biotechnology and Health Sciences, Wuyi University, Jiangmen, China. E-mail: jiangh@bnu.edu.cn, kzhang@gdut.edu.cn*
[b]*International Healthcare Innovation Institute (Jiangmen), Jiangmen, China*
[c]*School of Chemical Engineering and Light Industry, Guangdong University of Technology, Guangzhou, China*
[d]*College of Chemistry, Beijing Normal University, Beijing, China*

†Electronic supplementary information (ESI) available. CCDC 1939544 and 1939549. For ESI and crystallographic data in CIF or other electronic format see DOI: 10.1039/c9ob01649j

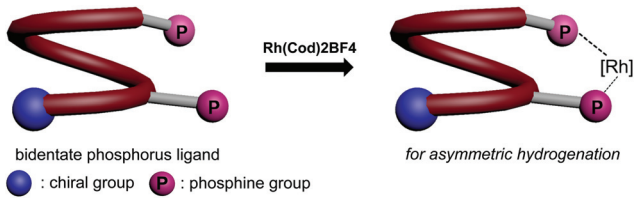

Fig. 1 Illustration of the chiral catalyst based on the chiral quinoline oligoamide foldamer.

the most commonly used ligands that asymmetric catalysts are highly dependent on and have attracted huge attention and made great progress in recent years.[28–30] Chiral phosphine ligands bearing three aryl substituents are an important class of structures for transition metal catalysts and have been applied in a number of asymmetric reactions because of their high levels of enantioselectivity and stability.[31] Hence, we designed and synthesized several bidentate phosphorus ligands bearing three aryl substituents based on quinoline oligoamide foldamers in which the (−)-camphanyl moiety was used as the chiral motif at the N-terminus of the foldamer because of its absolute induction of the *P* helix for quinoline oligoamide foldamers and commercial availability.[26] We expected that the bidentate ligands could coordinate with $Rh(cod)_2BF_4$ in a 1/1 ratio to form a cyclic Rh-complex which can be used for the asymmetric hydrogenation of α-dehydroamino acid esters with good conversions and enantioselectivities.

Initially, two achiral bidentate phosphorus ligands **L1** and **L2** bearing monomer **6** at the N-terminus and a 1,3-phenylenediphenylphosphino group at the C-terminus (Scheme 1 and the ESI†) of the foldamers were prepared to verify whether this kind of bidentate phosphorus ligand can coordinate with Rh $(cod)_2BF_4$. X-ray crystallographic analyses show that the structures of **L1** and **L2** span more than one helical turn with the

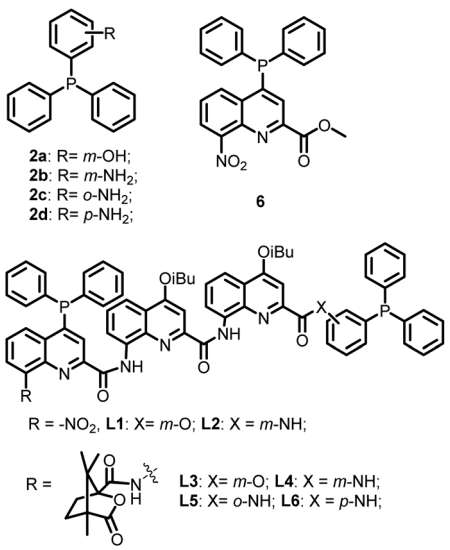

Scheme 1 The structures of the foldamer-based ligands **L1**–**L6**.

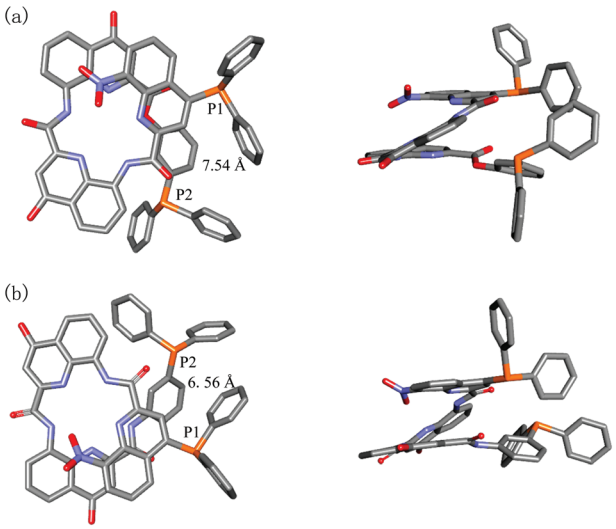

Fig. 2 Top view and side view of the crystal structures of ligands **L1** (a) and **L2** (b). All isobutyl side chains were omitted for clarity. C, gray; N, blue; O, red; H, white and P, orange.

two phosphorus groups located on the same face of the helices (Fig. 2). After the addition of one equivalent of $Rh(cod)_2BF_4$ to the solution of **L1** or **L2** in $CDCl_3$, ^1H NMR experiments showed that the original signals of **L1** and **L2** completely disappeared with the concomitant appearance of a set of new signals respectively, hinting at the formation of L1[Rh] (L[Rh] is short for $RhL(Cod)BF_4$, *e.g.*, L2[Rh], Fig. 3a) and L2[Rh] complexes (Fig. 3b). The upfield shifts of the amide hydrogens were observed for both L1[Rh] and L2[Rh], indicating the different shielding effects as a result of the formation of cyclic structures. Besides, the ^{31}P-signal patterns are one set of doublet of doublet peaks for L1[Rh] and two sets of doublet of doublet peaks for L2[Rh] (Fig. 3c), which are the characteristic P–P and P–Rh coupling constants (*e.g.*, L2[Rh], J_{P-P} = 29.16 Hz, J_{P-Rh} = 140.9, 143.4 Hz) that reveal the successful coordination between the phosphine ligands and the rhodium atoms that further illustrates the formation of the cyclic structures.[32] ESI-MS confirmed that the L1[Rh] and L2[Rh] complexes were obtained in a 1 : 1 stoichiometry according to the peaks of $[L[Rh]\text{-}BF_4^-]^+$ (Fig. S13 and S14†).

Then we attempted to investigate whether the two L[Rh] complexes can be used as active catalysts for the hydrogenation of α-dehydroamino acid esters and the hydrogenation reactions using L2[Rh] as the catalyst were performed under different conditions (Table S1†). The results showed that moderate conversions were detected when 2 mol% of L2[Rh] was used under 1 atm of H_2 for **1a–1g** in $CDCl_3$. Increasing the pressure to 10 atm enhanced the conversions for **1a–1g** from 20%–80% to 72%–98%. Complete conversions for **1a–1g** could be obtained by using 4 mol% of L2[Rh] as the catalyst under 7 atm of H_2 at room temperature. The hydrogenations of **1a–1g** in two other solvents, THF and toluene, were also conducted using 4 mol% of L2[Rh] as the catalyst under 7 atm of H_2 at room temperature and complete conversions were observed

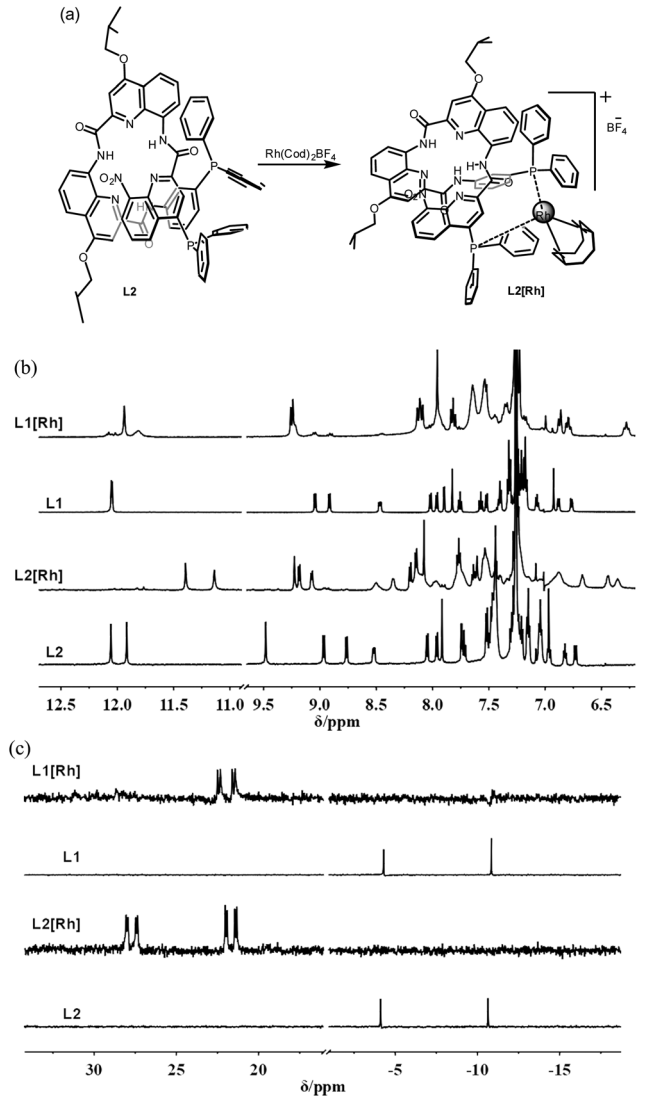

Fig. 3 (a) Coordination structure of L2[Rh], and (b) ^{1}H NMR and (c) ^{31}P NMR spectra of compounds **L1** and **L2**, and the produced metal complexes L1[Rh] and L2[Rh] in $CDCl_3$ at 298 K.

(Table S1 and Fig S22–42†). These results demonstrated that the L2[Rh] complex could be used as an efficient catalyst for the hydrogenation of α-dehydroamino acid esters. L1[Rh] was also evaluated under the same conditions mentioned above and the results of the hydrogenation revealed that L1[Rh] is also an effective catalyst for the hydrogenation reactions (Table S2†).

With these results in hand, we began to introduce the (−)-camphanyl moiety that can induce a complete *P* helix even for trimeric QOFs into the N-termini of **L1** and **L2**, and the chiral ligands **L3** and **L4** were synthesized (Scheme 1 and S1†). To clarify whether the large side chain can alter the chiral induction ability of the (−)-camphanyl group in the chiral ligands, the variable temperature (VT) ^{1}H NMR experiments of **L4** were carried out from 25 to −80 °C in CD_2Cl_2 and only one set of signals can be detected in the whole range of temperatures (Fig. S12†), hinting at the absolute helical sense bias of the (−)-camphanyl moiety for **L4**. The coordination of **L3** and **L4** with $Rh(cod)_2BF_4$ was studied by ^{1}H NMR, ^{31}P NMR and ESI-MS (Fig. S5–8, S15 and S16†), which were similar to those of **L1** and **L2**, indicating the successful coordination of the phosphorus atoms and the rhodium atom and the formation of the cyclic structures. The CD spectra of **L3**, **L4**, L3[Rh] and L4[Rh] were obtained in DCM (Fig. S18 and S19†) and strong positive signals can be observed in the absorption region of quinoline rings between 250 and 500 nm for all the ligands and L[Rh] complexes, which demonstrate the chiral induction of (−)-camphanyl for these compounds.

In order to investigate the ability of **L3** and **L4** to induce the enantioselectivity in Rh(I)-catalyzed asymmetric hydrogenation, the hydrogenation reactions of α-dehydroamino acid ester **1a** were performed under 7 atm of H_2 in $CDCl_3$, toluene and THF. The ligand **L3**, in which the 1,3-phenylenediphenylphosphino group at the C-terminus was connected to QOFs by an ester bond, displays full conversions in the three mentioned solvents but with low ee values (Table 1, entries 1–3, 4%–12%, Fig. S43–47†). However, the ligand **L4** connecting the 1,3-phenylenediphenylphosphino group at the C-terminus by an amide bond exhibits an increase in enantioselectivity up to 49% in $CDCl_3$ and 42% in toluene but only 10% in THF (Table 1, entries 4–6, Fig. S48–51†). These results not only revealed that the enantioselectivity greatly depends on the solvent used but also demonstrated that the amide bond at the C-terminus is beneficial for the enantioselectivity in asymmetric hydrogenation, which may be because the hydrogen bond between the amide hydrogen and the nitrogen atom in the adjacent quinoline ring enhanced the chiral transmission efficiency from the chiral foldamer to the produced metal complex that determined the enantioselectivity of hydrogenation.

Table 1 Optimization for asymmetric hydrogenation of methyl (*Z*)-2-acetamido-3-phenylacrylate[a]

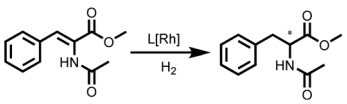

Entry	Ligand	Solvent	Conv. (%)	ee (%)
1	**L3**	$CDCl_3$	>98	8
2		THF	>98	4
3		Toluene	>98	12
4	**L4**	$CDCl_3$	>98	49
5		THF	76	10
6		Toluene	>98	42
7	**L5**[b]	$CDCl_3$	10	—
8		THF	6	—
9		Toluene	5	—
10	**L6**	$CDCl_3$	>98	0
11		THF	>98	3
12		Toluene	>98	11

[a] $[Rh(cod)_2]BF_4$: ligand : substrate = 4/4/100, 7 atm of H_2, room temperature, 12 h. The conversions were determined by ^{1}H NMR spectroscopy and the ee values were determined by chiral GC using a Varian Chirasil-L-Val column CP7495 (25 m × 0.25 mm). [b] The hydrogenation was performed under 15 atm of H_2 for **L5**.

Given that the structure and steric conformation of the reactive site in catalysts play an important role in the enantioselectivity of transition metal complex catalyzed asymmetric reactions,[12] we proposed to modulate the steric hindrance of the metal-binding site by changing the substituted position of the phenylenediphenylphosphino group to improve the enantioselectivity of the asymmetric hydrogenation. We expected that the *ortho*-substituted amino-phenylenediphenylphosphino group would increase the steric hindrance, which would enhance the enantioselectivity of the asymmetric hydrogenation of α-dehydroamino acid ester **1a**; however, the *para*-substituted amino-phenylenediphenylphosphino group decreased the steric hindrance resulting in lower enantioselectivity of the hydrogenation. To verify our concept, compounds **L5** and **L6** were designed and synthesized (Scheme 1 and S1†). The coordination ability of **L5** and **L6** with Rh $(cod)_2BF_4$ was tested in $CDCl_3$ and monitored by ^1H NMR and ESI-MS, which showed that the corresponding cyclic Rh-complex was formed for **L5** when 1.0 equivalent of Rh $(cod)_2BF_4$ was added (Fig. S9, S10 and S17†). The ^1H NMR spectra of **L6** and L6[Rh] showed that the signals of **L6** disappeared with the emergence of complex patterns of peaks (Fig. S11†), which revealed that maybe more than one kind of Rh-complex was formed in the solution. The CD spectra of **L5**, **L6**, L5[Rh] and L6[Rh] showed the chiral amplification of (−)-camphanyl to cyclic Rh-complexes (Fig. S20 and S21†).

The hydrogenation reaction of α-dehydroamino acid ester **1a** using L5[Rh] and L6[Rh] as the catalysts was conducted under the same conditions mentioned above to assess their reactivities and enantioselectivities. It is surprising that the steric hindrance of L5[Rh] is so large that the double bond in **1a** cannot coordinate with the catalytically active site, which resulted in the catalytic activity of L5[Rh] being lowered to a certain extent, even increasing the pressure of H_2 to 15 atm regardless of the solvent used (Table 1, entries 7–9, Fig. S52–54†). Complete conversions were obtained in the three solvents when L6[Rh] was used as the catalyst, but they were accompanied by rather low ee values of the hydrogenated product of **1a** probably because of the weak steric hindrance (Table 1, entries 10–12, Fig. S55–57†). The modification of the substituted position of the amino-phenylenediphenylphosphino group produced tremendous changes in enantioselectivities and conversions of asymmetric hydrogenation, which was indicative of the significance of the steric hindrance effect.

The results summarized in Table 1 show clearly that **L4** exerted the best enantioselectivity in the four chiral foldamer-based ligands and $CDCl_3$ was the best solvent used in which 100% conversion and 49% ee value can be obtained for the hydrogenation product of **1a**. Therefore, some other electron-efficient or electron-deficient α-dehydroamino acid esters were applied in the asymmetric hydrogenation under 7 atm of H_2 in the presence of 4 mol% L4[Rh] to further assess the reactivity and enantioselectivity of L4[Rh] and the results are shown in Table 2 (Fig. S58–69†). All the hydrogenation reactions proceeded smoothly with complete conversions and moderate ee values (39%–54%). High ee values were provided by the electron-deficient substrates (Table 2, entries 6 and 7) compared with the electron-efficient substrates (Table 2, entries 1–5). Reducing the dosage of L4[Rh] to 2 mol% for **1f** and **1g** did not affect the ee values of the hydrogenation products (Table 2, entries 6 and 7).

Table 2 Asymmetric hydrogenation of α-dehydroamino acid esters[a]

Entry	Substrate (R)	Conv. (%)	ee (%)
1	**1a** (H)	>98	49
2	**1b** (2-OMe)	>98	47
3	**1c** (3-OMe)	>98	49
4	**1d** (4-OMe)	>98	39
5	**1e** (2-Me)	>98	48
6	**1f** (4-F)	>98	53 (51)[b]
7	**1g** (3-Cl)	>98	54 (48)[b]

[a] $[Rh(cod)_2]BF_4$: **L4** : substrate = 4/4/100, 7 atm of H_2, room temperature, 12 h. The conversions were determined by ^1H NMR spectroscopy and the ee values were determined by GC using a Varian Chirasil-L-Val column CP7495 (25 m × 0.25 mm). [b] The catalyst loading for the ee values in parentheses is 2 mol%.

Conclusions

In conclusion, we have synthesized a series of chiral bidentate phosphoric ligands based on single-handed quinoline oligoamide foldamers, which can coordinate with $Rh(cod)_2BF_4$ in a 1 : 1 stoichiometry and the produced rhodium complex can be used for asymmetric hydrogenations. The enantioselectivity and reactivity of the hydrogenation reaction is highly dependent on the chirality of the metallocycle that is transferred from the helical chirality and the structure and microenvironment of the catalytically active site. Complete conversions and moderate enantioselectivity were obtained in the hydrogenation of α-dehydroamino acid esters when L4[Rh] was used as the catalyst, which demonstrated that the chiral foldamers can be used as a platform for the asymmetric reaction. This work is expected to trigger further investigation of aromatic foldamers for the development of chiral ligands for asymmetric catalysis.

Conflicts of interest

There are no conflicts to declare.

Acknowledgements

We acknowledge the financial supports from the 973 Program (2015CB856502) and the National Natural Science Foundation of China (21672026).

Notes and references

1 I. Huc and H. Jiang, Organic Foldamers and Helices, in *Supramolecular Chemistry: From Molecules to Nanomaterials*, ed. P. A. Gale and J. W. Steed, John Wiley & Sons Ltd., Chichester, UK, 2012, pp. 2183–2206.
2 A. J. Boersma, R. P. Megens, B. L. Feringa and G. Roelfes, *Chem. Soc. Rev.*, 2010, **39**, 2083–2092.
3 J. Steinreiber and T. R. Ward, *Coord. Chem. Rev.*, 2008, **252**, 751–766.
4 N. Delsuc, T. Kawanami, J. Lefeuvre, A. Shundo, H. Ihara, M. Takafuji and I. Huc, *J. Am. Chem. Soc.*, 2008, **130**, 13210–13211.
5 C. Dolain, C. Zhan, J.-M. Léger, L. Daniels and I. Huc, *J. Am. Chem. Soc.*, 2005, **127**, 2400–2401.
6 R. A. Smaldone and J. S. Moore, *J. Am. Chem. Soc.*, 2007, **129**, 5444–5450.
7 J. M. Heemstra and J. S. Moore, *J. Am. Chem. Soc.*, 2004, **126**, 1648–1649.
8 D. Bécart, V. Diemer, A. Salaün, M. Oiarbide, Y. R. Nelli, B. Kauffmann, L. Fischer, C. Palomo and G. Guichard, *J. Am. Chem. Soc.*, 2017, **139**, 12524–12532.
9 R. Sambasivan and Z. T. Ball, *Angew. Chem., Int. Ed.*, 2012, **51**, 8568–8572.
10 R. Sambasivan and Z. T. Ball, *J. Am. Chem. Soc.*, 2010, **132**, 9289–9291.
11 J. Lu and P. H. Toy, *Chem. Rev.*, 2009, **109**, 815–838.
12 R. P. Megens and G. Roelfes, *Chem. – Eur. J.*, 2011, **17**, 8514–8523.
13 M. Reggelin, M. Schultz and M. Holbach, *Angew. Chem., Int. Ed.*, 2002, **41**, 1614–1617.
14 A. Desmarchelier, X. Caumes, M. Raynal, A. Vidal-Ferran, P. W. van Leeuwen and L. Bouteiller, *J. Am. Chem. Soc.*, 2016, **138**, 4908–4916.
15 T. Yamamoto, R. Murakami and M. Suginome, *J. Am. Chem. Soc.*, 2017, **139**, 2557–2560.
16 Y. Yoshinaga, T. Yamamoto and M. Suginome, *ACS Macro Lett.*, 2017, **6**, 705–710.
17 T. Yamamoto, Y. Akai and M. Suginome, *Angew. Chem., Int. Ed.*, 2014, **53**, 12785–12788.
18 Y. Z. Ke, Y. Nagata, T. Yamada and M. Suginome, *Angew. Chem., Int. Ed.*, 2015, **54**, 9333–9337.
19 T. Yamamoto, Y. Akai, Y. Nagata and M. Suginome, *Angew. Chem., Int. Ed.*, 2011, **50**, 8844–8847.
20 M. Karras, M. Dabrowski, R. Pohl, J. Rybacek, J. Vacek, L. Bednarova, K. Grela, I. Stary, I. G. Stara and B. Schmidt, *Chem. – Eur. J.*, 2018, 24, 10994–10998.
21 M. J. Narcis and N. Takenaka, *Eur. J. Org. Chem.*, 2014, 21–34.
22 N. Ousaka, T. Yamaguchi and E. Yashima, *Chem. Lett.*, 2014, **43**, 512–514.
23 H. Jiang, J. Léger and I. Huc, *J. Am. Chem. Soc.*, 2003, **125**, 3448–3449.
24 D. Zheng, L. Zheng, C. Yu, Y. Zhan, Y. Wang and H. Jiang, *Org. Lett.*, 2019, **21**, 2555–2559.
25 L. Zheng, Y. Zhan, C. Yu, F. Huang, Y. Wang and H. Jiang, *Org. Lett.*, 2017, **19**, 1482–1485.
26 A. M. Kendhale, L. Poniman, Z. Dong, K. Laxmi-Reddy, B. Kauffmann, Y. Ferrand and I. Huc, *J. Org. Chem.*, 2011, **76**, 195–200.
27 L. Zheng, C. Yu, Y. Zhan, X. Deng, Y. Wang and H. Jiang, *Chem. – Eur. J.*, 2017, **23**, 5361–5367.
28 Y. M. He, Y. Feng and Q. H. Fan, *Acc. Chem. Res.*, 2014, **47**, 2894–2906.
29 P. J. Guiry and C. P. Saunders, *Adv. Synth. Catal.*, 2004, **346**, 497–537.
30 W. Zhao, D. Yang and Y. Zhang, *Chin. J. Org. Chem.*, 2016, **36**, 2301.
31 M. Xue, J. Li, J. Peng, Y. Bai, G. Zhang, W. Xiao and G. Lai, *Appl. Organomet. Chem.*, 2014, **28**, 120–126.
32 P. W. van Leeuwen, D. Rivillo, M. Raynal and Z. Freixa, *J. Am. Chem. Soc.*, 2011, **133**, 18562–18565.